THE JOURNAL OF PHYSICAL CHEMISTRY B

Article

pubs.acs.org/JPCB

Characterization of the Chemical Composition of Polyisobutylene-Based Oil-Soluble Dispersants by Fluorescence

Solmaz Pirouz, Yulin Wang, J. Michael Chong, and Jean Duhamel*

Waterloo Institute for Nanotechnology, Institute for Polymer Research, Department of Chemistry, University of Waterloo, Waterloo, ON N2L 3G1, Canada

Supporting Information

ABSTRACT: A novel methodology based on fluorescence quenching measurements is introduced to determine quantitatively the amine content of polyisobutylene succinimide (PIBSI) dispersants used as engine oil-additives. To this end, a series of five PIBSI dispersants were prepared by reacting 2 mol equiv of polyisobutylene succinic anhydride (PIBSA) with 1 mol equiv of hexamethylenediamine (HMDA), diethylenetriamine, triethylenetetramine, tetraethylenepentamine, and pentaethylenehexamine to yield the corresponding *b*-PIBSI dispersants. After having demonstrated that the presence of hydrogen bonds between the polyamine linker and the succinimide carbonyls of the dispersants prevents the quantitative analysis of the ^{1}H NMR and FTIR spectra of the dispersants to determine their chemical composition, alternative procedures based on gel permeation chromatography (GPC) and fluorescence quenching were implemented to estimate the amine content of the *b*-PIBSI dispersants. Taking advantage of the doubling in size that occurs when 2 mol of PIBSA are reacted with 1 mol of HMDA, a combination of GPC and FTIR was employed to follow how the chemical composition and molecular weight distribution of the polymers produced evolved with the reaction of PIBSA and HMDA mixed at different molar ratios. These experiments provided the PIBSA-to-HMDA molar ratio yielding the largest *b*-PIBSI dispersants and this molar ratio was then selected to prepare the four other dispersants. Having prepared five *b*-PIBSI dispersants with well-defined secondary amine content, the fluorescence of the succinimide groups was found to decrease with increasing number of secondary amines present in the polyamine linker. This result suggests that fluorescence quenching provides a valid method to determine the chemical composition of *b*-PIBSI dispersants which is otherwise difficult to characterize by standard ^{1}H NMR and FTIR spectroscopies.

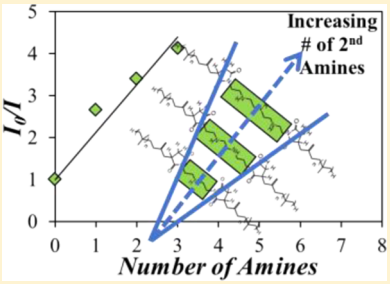

INTRODUCTION

Dispersants, detergents, viscosity modifiers, antiwear, and antioxidation components are chemicals that are purposely added to engine oils to improve the oil performance during the operation of gasoline and diesel engines. These additives are designed to improve engine efficiency and durability. Dispersants represent the most important family of chemical additives and they have been used in engine oils since the 1950s.[1−3] They constitute up to 10 wt % of an engine oil formulation and around 50 wt % of the total chemical additives found in the oil.[4] They work by dispersing oil-insoluble combustion byproducts such as soot and sludge generated during the normal operation of the engine.

Soot or ultrafine particles (UFPs) are either carbon-rich and/or metallic in nature. Typically, these particles, which result from the incomplete oxidation of fuel during ignition, are smaller than 100 nm in diameter and can be released to the air with the exhaust gases.[5] Since released UFPs are responsible for a number of ailments that can lead to heart and lung failure, governmental regulations have been issued to reduce UFPs emission.[6−8] To this end, diesel and gasoline engine manufacturers circulate the exhaust gas back into the oil[9] where UFPs remain trapped before the exhaust gas is released to the air, in turn, resulting in higher concentrations of UFPs in the oil that promote UFPs aggregation.[10] UFPs aggregation is due to the polar groups formed on the surface of UFPs following fuel oxidation. The UFPs aggregate into large particles (LPs) with a diameter on the order of 1 μm to minimize their surface exposure to the oil. The LPs eventually precipitate out of solution generating the soot that is detrimental to the good operation of the engine. Dispersants added to the oil prevent the formation of LPs. They adsorb onto the surface of UFPs, stabilizing them by a steric or electrostatic mechanism which reduces the aggregation of UFPs into LPs.[2,11,12]

Polyisobutylene succinimide dispersants (PIBSI) are the most common nonionic dispersants used in the oil industry. In fact, the ability of polyisobutylene (PIB) to interact with apolar liquids has been employed in several other applications that include the synthesis of PIB-containing cross-linked acrylate networks capable of absorbing crude oil[13] or dispersants that can stabilize pigments[14] or carbon nanotubes.[15] PIBSI were initially developed by Le Suer and Stuart in 1966.[16−19] The preparation of PIBSI begins by generating a polyisobutylene

Received: January 27, 2014
Revised: March 14, 2014
Published: March 14, 2014

   dx.doi.org/10.1021/jp5009576 | J. Phys. Chem. B 2014, 118, 3899−3911

Scheme 1. Synthesis of Succinimide Dispersants

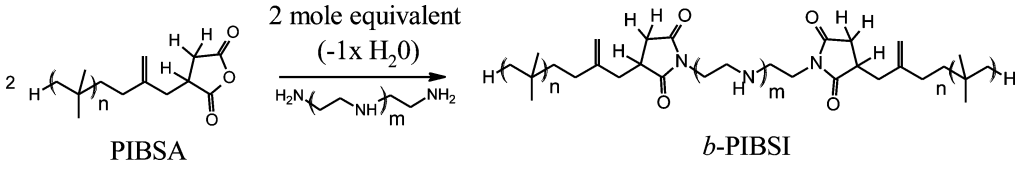

chain terminated at one end with a succinic anhydride group (PIBSA). PIBSA can be prepared by an Alder-ene reaction between the terminal double bond located at the end of polyisobutylene and maleic anhydride at high temperature.[17,20] Reaction of PIBSA with a polyamine in a 1:1 or 1:2 polyamine:PIBSA ratio generates *mono*-PIBSI (*m*-PIBSI) and *bis*-PIBSI (*b*-PIBSI) dispersants, respectively.[21−24] Since increasing the number of secondary amines in the polyamine core of PIBSI dispersants results in a stronger binding onto UFPs, using a large number of secondary amines should theoretically lead to better oil performance. In practice, however, the secondary amines make the oil more basic which is detrimental to the integrity of the engine seals. The basicity of the oil can be reduced through postmodification of the PIBSI-dispersants with ethylene carbonate or boric acid.[25,26] These considerations underline the importance of knowing the secondary amine content of PIBSI-dispersants. As it turns out, this information is not easily obtained, as characterization techniques based on FTIR or ^{1}H NMR spectroscopies[22,27] which are typically used by chemists to determine the chemical composition of unknown compounds are not suitable for this purpose. The experiments described hereafter suggest that interactions between the succinimide groups and the secondary amines is responsible for complicating the analysis of the chemical composition of PIBSI-dispersants by FTIR or ^{1}H NMR spectroscopies.

Taking advantage of the inherent fluorescence of the succinimide moiety of PIBSI-dispersants and its efficient quenching by secondary amines, this study establishes a quick and straightforward analytical method to characterize the secondary amine content of PIBSI-dispersants based on the fluorescence quenching of the succinimide group. Considering how important the secondary amine content of PIBSI-dispersants is to understand their solution properties, this work is expected to interest scientists aiming to design oil-soluble dispersants with improved properties.

EXPERIMENTAL SECTION

Chemicals. Acetone (HPLC grade, Caledon), hexane (HPLC grade, Caledon), xylene (reagent grade, 98.5%, EMD), tetrahydrofuran (THF, HPLC grade, Caledon), dodecane (anhydrous, 99%, Sigma-Aldrich), and 2-dodecanone (GC grade, 97%, Sigma-Aldrich) were used as received. The chemicals hexamethylenediamine (HMDA, 98%), diethylenetriamine (DETA, 99%), triethylenetetramine (TETA, 97%), tetraethylenepentamine (TEPA, technical grade), pentaethylenehexamine (PEHA, technical grade), octylamine (99%), 1-pyrenemethylamine hydrochloride ($PyNH_2$−HCl, 95%), *N*-methylsuccinimide (*N*-MSI, 99%), butylamine (BUA, 99%), diethylamine (DEA, 99.5%), and triethylamine (TEA, 99.5%) were purchased from Sigma-Aldrich and were employed without further purification. Polyisobutylene succinic anhydride (PIBSA) was supplied by Imperial Oil.

Proton Nuclear Magnetic Resonance (^{1}H NMR). A Bruker 300 MHz high resolution NMR spectrometer was used to acquire the ^{1}H NMR spectra of the dispersants in deuterated chloroform ($CDCl_3$, 99.8%, Cambridge Isotope Laboratory Inc.). A sample concentration of about 10 mg/mL was used to obtain ^{1}H NMR spectra of the polymer samples with a reasonable signal-to-noise (S/N) ratio.

Fourier Transform Infrared (FTIR). All FTIR spectra were obtained with a Bruker Tensor 27 FTIR spectrometer using NaCl FTIR cells. Deuterated chloroform ($CDCl_3$, 99.8%, Cambridge Isotope Laboratory Inc.) was used as solvent in all sample preparations. Polymer solutions prepared with $CDCl_3$ were deposited dropwise onto the NaCl FTIR cell. The solvent was evaporated under a stream of nitrogen leaving behind a polymer film. All samples had an absorbance of less than 1 to optimize the S/N ratio.

Gel Permeation Chromatography (GPC). A Viscotek GPC max VE 2001 instrument equipped with a Viscotek TDA 305 triple detector array comprised of a refractive index, viscosity, and light scattering detector was used. The samples were passed through a divinylbenzene mixed bed (8.0 mm × 300 mm) Polyanalytik column. Tetrahydrofuran (THF) was used as the solvent at a flow rate of 1.0 mL/min. All samples were filtered using a 0.2 μm Millipore poly(tetrafluoroethylene) (PTFE) filter before injection and the sample concentration was less than 10 mg/mL. Because of their low molecular weight (<6000 g·mol^{-1}), the polyisobutylene samples used in this study did not scatter light strongly enough to yield a reliable light scattering signal and the light scattering detector of the GPC instrument could not be used to determine their absolute molecular weight. Instead the GPC instrument determined the apparent molecular weight of the polyisobutylene samples as it was calibrated with polystyrene standards.

UV−Visible Spectrophotometer (UV−Vis). Absorbances were measured on a Cary 100 UV−visible spectrophotometer with quartz cells having a 0.1−100 mm path length. Absorbances were measured in the 200−600 nm wavelength range.

Steady-State Fluorescence. A Photon Technology International (PTI) LS-100 steady-state fluorometer equipped with an Ushio UXL-75Xe xenon arc lamp and a PTI 814 photomultiplier detection system was used to acquire the fluorescence spectra.

Time-Resolved Fluorescence. An IBH time-resolved fluorometer fitted with a 340 nano-LED light source was used to acquire the fluorescence decays. Light scattering and background corrections were applied to fit the fluorescence decays. The fluorescence decay curves of the PIBSI-dispersants were fitted by a sum of exponentials shown in eq 1,

$$i(t) = \sum_{i=1}^{n_{exp}} a_i \times \exp(-t/\tau_i) \quad (1)$$

where n_{exp} represents the number of exponentials used and the parameters a_i and τ_i represent the amplitude and decay time of the ith exponential, respectively. The decay fits were considered to be good if the χ^2 value was smaller than 1.30 and the

dx.doi.org/10.1021/jp5009576 | J. Phys. Chem. B 2014, 118, 3899−3911

residuals and the autocorrelation of the residuals were randomly distributed around zero.

Synthesis of the Polyisobutylene Succinimide (PIBSI) Dispersants. The polyisobutylene succinimide (PIBSI) dispersants were synthesized by reacting different amine derivatives with PIBSA using PIBSA-to-polyamine mole ratios of 1:1 or 2:1 in order to generate *mono*-PIBSI (*m*-PIBSI) and *bis*-PIBSI (*b*-PIBSI) dispersants, respectively. Scheme 1 describes the reaction between the succinic anhydride of PIBSA and the primary amine of the polyamines to generate the *b*-PIBSI dispersants.[21,23] In the current study, octylamine, diethylenetriamine (DETA), triethylenetetramine (TETA), tetraethylenepentamine (TEPA), pentaethylenehexamine (PEHA), and hexamethylenediamine (HMDA) were used as polyamines and their chemical structures are given in Table 1.

Table 1. Chemical Structures of the Amine Derivatives Used to Prepare the PIBSI Dispersants

polyamine	chemical structure
octylamine	$CH_3(CH_2)_7NH_2$
diethylenetriamine (DETA)	$H_2N(CH_2CH_2{-}NH)_2H$
triethylenetetramine (TETA)	$H_2N(CH_2CH_2{-}NH)_3H$
tetraethylenepentamine (TEPA)	$H_2N(CH_2CH_2{-}NH)_4H$
pentaethylenehexamine (PEHA)	$H_2N(CH_2CH_2{-}NH)_5H$
hexamethylenediamine (HMDA)	$H_2N(CH_2)_6NH_2$

All PIBSI-dispersants were synthesized according to Scheme 1 using a same molar ratio of succinic anhydride of PIBSA to primary amines of the polyamine. The synthesis of *b*-PIBSI-TEPA is described in more detail as an example. Before conducting the reaction presented in Scheme 1, PIBSA as supplied by Imperial Oil was precipitated to remove low molecular weight impurities that might be present in the sample. The crude PIBSA sample (10 g) was dissolved in 10 mL of hexane at 50 °C. Then the warm PIBSA solution was gradually added into 500 mL of cold acetone where it precipitated. The PIBSA suspension was centrifuged at room temperature for 20 min. The supernatant was discarded, and the pellet was dried overnight at 60−70 °C in a vacuum oven.

Since the succinic anhydride of PIBSA is moisture sensitive and can react with water to yield succinic acid which is much less reactive than succinic anhydride, dehydration of the succinic acid was carried out. To this end, PIBSA purified by precipitation from acetone (2 g, 0.66 mmol succinic anhydride equivalent) was dissolved in 20 mL xylene and placed into a two-neck round-bottom flask equipped with a Dean−Stark apparatus to remove the water generated during the dehydration conducted at 130−140 °C in refluxing xylene for 10 h under nitrogen atmosphere. Successful dehydration was confirmed by comparison in Figure 1 of the FTIR absorption of partially hydrated PIBSA (trace a) with that of dehydrated PIBSA (trace b). The FTIR spectrum of partially hydrated PIBSA shows two absorptions bands at 1705 and 1785 cm^{-1} due to the carbonyl groups of succinic acid and succinic anhydride (SA), respectively. After dehydration, the absorption at 1705 cm^{-1} disappeared, demonstrating that all succinic acids were converted back to their SA form.

After having left the PIBSA solution refluxing in xylene for 10 h, TEPA (0.063 g, 0.33 mmol) was added to achieve a 1:2 polyamine-to-PIBSA ratio and the reaction was left to proceed at the same temperature under nitrogen for another 10 h. When the reaction was complete, the reaction mixture

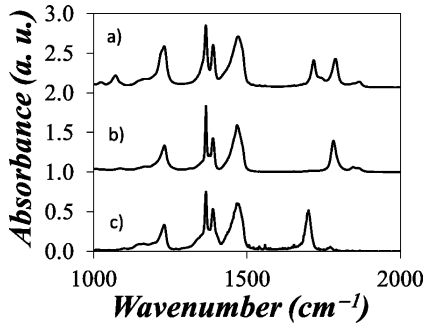

Figure 1. FT-IR spectra of (a) partially hydrated PIBSA, (b) dehydrated PIBSA, and (c) *b*-PIBSI-TEPA.

containing the product was washed three times with 30 mL of 1 M HCl, 1 M NaOH, 0.5 M $NaHCO_3$, and Milli-Q water. The product was then dried overnight at 70 °C in a vacuum oven. FTIR spectroscopy was used to confirm the successful synthesis of *b*-PIBSI-TEPA. Comparison of the FTIR spectrum of *b*-PIBSI-TEPA (trace c in Figure 1) with that of PIBSA (trace b) shows the appearance of a new absorption band at 1705 cm^{-1} in Trace c due to the carbonyl groups of the succinimide ring and the disappearance of the band at 1785 cm^{-1} in Trace b. *b*-PIBSI-DETA, *b*-PIBSI-TETA, *b*-PIBSI-TEPA, *b*-PIBSI−PEHA, *b*-PIBSI-HMDA, and *m*-PIBSI-octylamine all showed similar FTIR spectra (see Figure S1 in Supporting Information).

The formation of secondary amides is unlikely during the preparation of the *b*-PIBSI dispersants. If this were the case, an absorption band at 1640 cm^{-1}, which is clearly absent in the FTIR spectrum of *b*-PIBSI-TEPA, would appear in the FTIR spectra, as was observed after the synthesis of *m*-PIBSI-TEPA (see Figure S2 in Supporting Information). The reaction with a 2:1 molar ratio of TEPA:SA led to the formation of succinamide bonds instead of forming the desired succinimide ring.

Synthesis of Bis(methyl succinimide)−DETA (b-MSI-DETA). Bis(methyl succinimide)−DETA (*b*-MSI-DETA) was prepared by reacting 3 mol equiv of methylsuccinic anhydride (MSA) with 1 mol equiv of DETA in refluxing xylene at 130−140 °C according to Scheme 2. A typical reaction proceeded as

Scheme 2. Reaction of MSA and DETA To Yield *b*-MSI-DETA

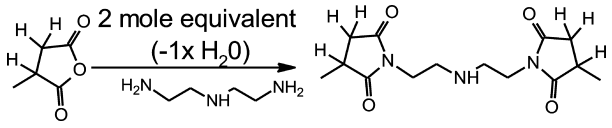

follows. MSA (0.5 g, 4.4 mmol) and DETA (0.23 g, 2.2 mmol) were dissolved in 10 mL of xylene. The reaction mixture was added in a two neck round-bottom flask equipped with a Dean−Stark trap, water condenser, and a nitrogen inlet and outlet to remove the water generated during the reaction conducted at 130−140 °C for 20 h.

After the reaction, 50 mL of xylene was added to the 10 mL reaction mixture. The 60 mL solution was washed separately with 10 mL of 0.5 M HCl solution, 10 mL of 0.5 M $NaHCO_3$, and 10 mL of Milli-Q water. Each extraction was repeated three times in order to remove the unreacted DETA. The organic fraction was collected. After the extractions were completed,

dx.doi.org/10.1021/jp5009576 | J. Phys. Chem. B 2014, 118, 3899−3911

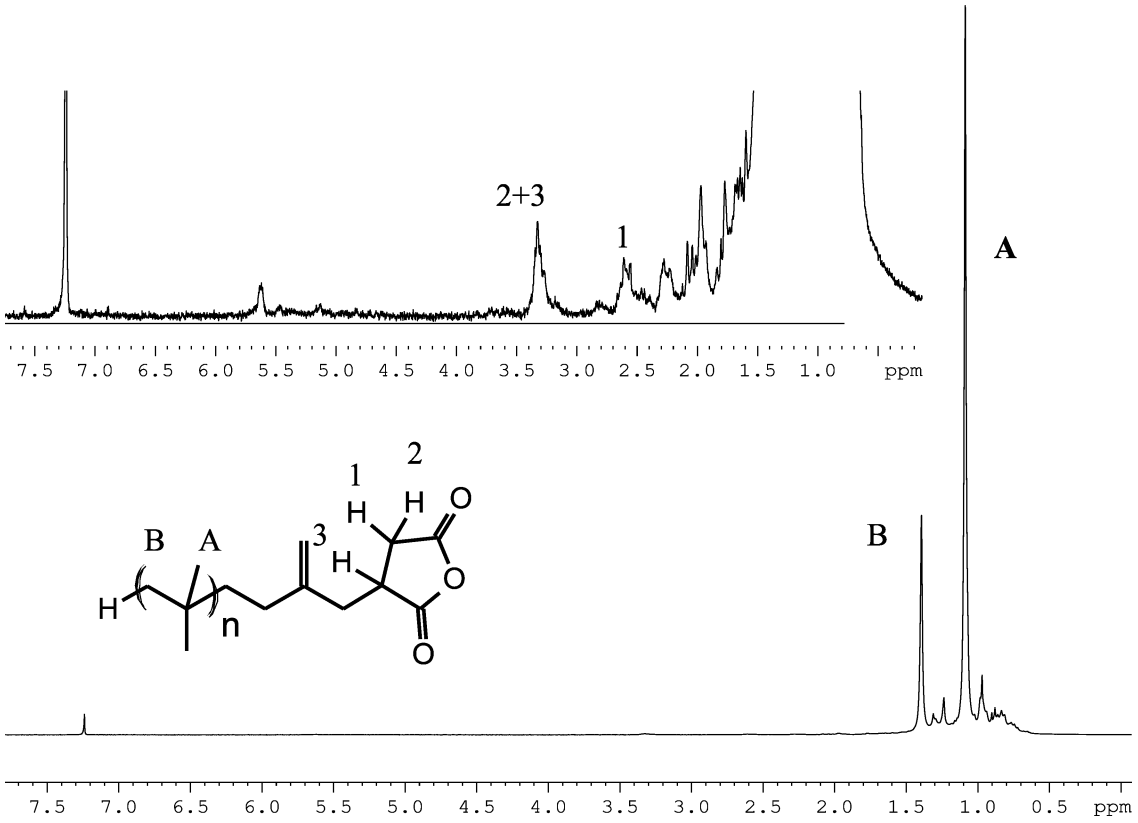

Figure 2. ^{1}H NMR spectrum of PIBSA.

the final product was dried in a vacuum oven. Since *b*-MSI-DETA is water-soluble, the yield after the three extractions was low around 10%.

Synthesis of Mono-PIBSI−Pyrenemethylamine (m-PIBSI-PyNH$_2$). 1-Pyrenemethylamine hydrochloride (PyNH$_2$·HCl) (0.302 g, 1.11 mmol) was dissolved in water (280 mL) and transferred to a separatory funnel. After addition of three NaOH pellets to the solution, PyNH$_2$ was extracted using hexanes (∼100 mL) and deionized water. Finally, the extracted PyNH$_2$ was dried in a vacuum oven at 60 °C for 2−3 h.[28]

PIBSA (1 g, 0.33 mmol equiv of SAH units) was dissolved in dodecane (8 mL) and placed in a two-neck round-bottom flask equipped with a Dean−Stark apparatus. The solution was heated at 180 °C for 8 h under nitrogen atmosphere to convert the succinic acid in the polymer to its anhydride form, and the dehydration process was monitored by FTIR (see Figure 1). After 8 h, an excess of PyNH$_2$ (185 mg, 0.80 mmol) was added and the temperature was kept at 180 °C for another 14 h. The final product was then dissolved in hexane and precipitated in acetone 5−6 times to remove all unreacted PyNH$_2$. The precipitated product was dried in a vacuum oven at 80−90 °C overnight.

RESULTS AND DISCUSSION

The succinimide moiety of PIBSI-dispersants is known to fluoresce.[29−32] Since secondary and tertiary amines are known quenchers of fluorescence,[33] it was reasoned that the quenching of succinimide by amines might provide a novel, rapid, and straightforward analytical method to characterize the chemical composition of *b*-PIBSI-dispersants in terms of the number of secondary amines per gram of dispersant. To this end, a series of *b*-PIBSI dispersants of known chemical composition needed to be synthesized and characterized. The chemical composition of PIBSA was determined by ^{1}H NMR, FTIR, UV−vis absorption, and a procedure based on GPC analysis. Knowledge of the chemical composition of PIBSA enabled the preparation of reaction mixtures that contained the correct molar ratio of succinic anhydride to primary amines that ensured the successful synthesis of a series of *b*-PIBSI-dispersants with a well-defined content of secondary amines. Attempts at determining the chemical composition of the *b*-PIBSI-dispersants by ^{1}H NMR and FTIR were inconclusive, however, certainly due to the unavoidable association of the dispersants in the solid state or in organic solvents that complicated the quantitative analysis of the ^{1}H NMR and FTIR spectra. Steady-state and time-resolved fluorescence measurements appeared to be impervious to these complications yielding a linear increase in quenching efficiency of the fluorescent succinimide units with increasing number of secondary amines. The following describes how these experiments were conducted.

Proton Nuclear Magnetic Resonance (^{1}H NMR). The assignment of the ^{1}H NMR spectrum of PIBSA was done by comparing it to that of methyl succinic anhydride (SA) shown in Figure S3 in Supporting Information. As shown in Figure S3, protons **1** and **2** of MSA do not have identical chemical shifts since they are diastereotopic. Protons **1** and **2** appear at 2.6 and 3.2 ppm, respectively, due to the rigid ring structure and the presence of the carbonyl groups in the SA cycle. Proton **3** overlaps proton **2**, and it is strongly deshielded by the methyl group of MSA. Protons **4** are represented as a doublet at 1.45 ppm. The single peaks at 1.5 and 7.25 ppm are due to the presence of residual water and chloroform in the sample, respectively.

dx.doi.org/10.1021/jp5009576 | J. Phys. Chem. B 2014, 118, 3899−3911

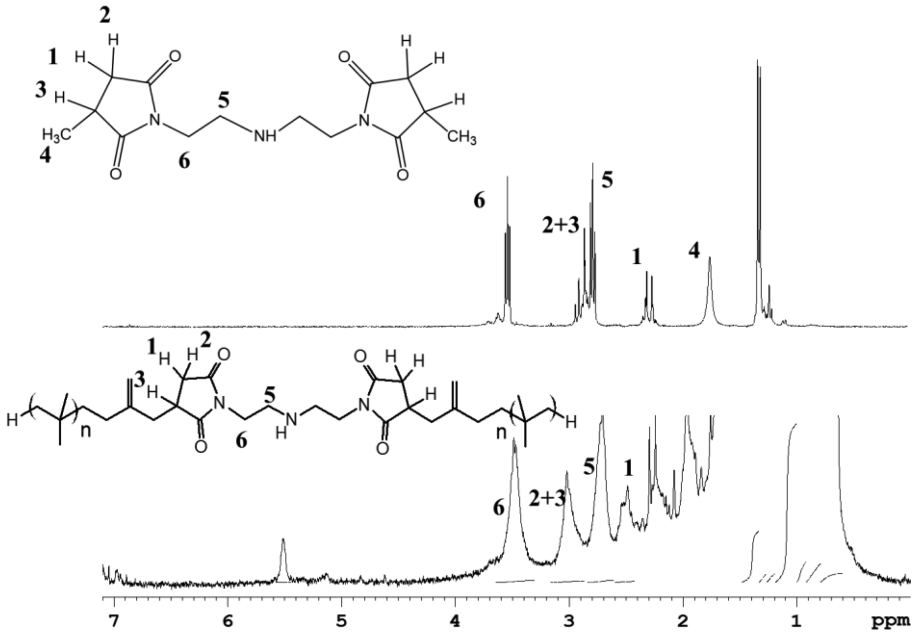

Figure 3. ^{1}H NMR spectrum of *b*-MSI-DETA (top) and *b*-PIBSI-DETA (bottom) (300 MHz, $CDCl_3$).

The ^{1}H NMR spectrum of PIBSA is shown in Figure 2. The SA protons of PIBSA are expected to have similar chemical shifts as those of protons **1**, **2**, and **3** in MSA. In the ^{1}H NMR spectrum of PIBSA, the peaks at 2.6 and 3.3 ppm represent the protons in the succinic anhydride ring. The peaks at 1.1 and 1.4 ppm represent, respectively, the methyl and the methylene protons of the PIB backbone obtained in a 3:1 ratio. Finally, the peak at 5.6 ppm may be due to the presence of vinylidene groups, which were generated during the cationic polymerization of PIB and did not react with maleic anhydride during the Alder-ene reaction. The sharp peak at 7.3 ppm is due to chloroform. The ratio of the integrals of the peaks at 1.4 and 3.3 ppm were used to calculate the average number of IB monomers (N_{IB}) in a PIBSA molecule per SA moiety (N_{SA}). The N_{SA}/N_{IB} ratio was found to be equal to 1:55 ± 2.

The ^{1}H NMR peak assignment for the *b*-PIBSI samples was done as follows. The polar core of the *b*-PIBSI dispersants carried different numbers of secondary amines depending on the polyamine used in the synthesis. Amine protons usually yield broad peaks in the ^{1}H NMR spectrum whose integration cannot be relied upon for quantitative analysis. Bis(methyl succinimide)diethyltriamine (*b*-MSI-DETA) was used as a model compound to help with the peak assignment of the ^{1}H NMR spectrum of *b*-PIBSI-DETA.

When MSA was reacted with DETA, the succinic anhydride proton **1** and the overlapping protons **2** and **3** shifted upfield from 3.3 and 2.6 ppm to 2.9 and 2.4 ppm, respectively (Figure 3). This shift is due to the substitution of the oxygen in the SA ring by the less electronegative nitrogen atom. Furthermore, new peaks appeared at 3.5 and 2.8 ppm due to the ethylene protons **5** and **6** in the DETA core of *b*-MSI-DETA. Comparison of the ^{1}H NMR spectra of *b*-PIBSI-DETA and *b*-MSI-DETA shows that the peaks at 2.7 and 3.5 ppm are due to the protons **6** and **5** of the ethylene segments of the polyamine linker whereas the peaks at 2.5 and 3.0 ppm are due to the succinimide ring protons **1** and **2** + **3** of *b*-PIBSI-DETA. The peaks at 1.4 and 1.1 ppm (not shown in the zoomed-in ^{1}H NMR spectra in Figure 3) represent the methylene and methyl protons of the PIB backbone, respectively. The sharp peaks at 2.25 and 2.3 ppm are due to traces of xylene.

The chemical composition of *b*-PIBSI-DETA was determined in terms of the number of succinimide moieties (N_{SI}) per number of isobutylene monomers (N_{IB}) by taking the ratio of the integrals of the peaks at 3.5 and 1.4 ppm in the ^{1}H NMR spectrum shown in the bottom panel of Figure 3. An N_{SI}/N_{IB} ratio of 1:32 ± 1 was obtained, similar to that of all other *b*-PIBSI samples and much smaller than the N_{SA}/N_{IB} ratio of 1:55 ± 2 found for PIBSA. This discrepancy in chemical composition between PIBSA and the *b*-PIBSI dispersant could be due to the purification procedure that might selectively eliminate the PIB-rich fraction of the *b*-PIBSI samples or some unexplained spectroscopic artifact due to H-bonding of the secondary amines in the polar core which might affect the peak intensities in the ^{1}H NMR spectra.

Fourier Transform Infrared (FTIR). FTIR spectroscopy was also used to determine the chemical composition of PIBSA using a calibration curve established by Walch and Gaymans whose expression is given in eq 2.[25] This calibration curve relates the N_{SA}/N_{IB} ratio of the number of SA groups to isobutylene (IB) units with the ratio of the FTIR absorbance at 1785 and 1390 cm^{-1}.

$$\frac{N_{SA}}{N_{IB}} = 0.024 \times \frac{\text{abs}(1785\ \text{cm}^{-1})}{\text{abs}(1390\ \text{cm}^{-1})} \quad (2)$$

The N_{SA}/N_{IB} ratio was found to equal 1:49 ± 1 for PIBSA, implying that the PIBSA sample contained one succinic anhydride unit per 49 isobutylene units. This result agrees with the ratio of 1:55 ± 2 found by ^{1}H NMR. Theoretically, the FTIR spectra can also be used to determine the chemical composition of PIBSI dispersants. A similar calibration curve whose expression is given in eq 3 was established to relate the ratio of the moles of IB units per succinimide (SI) for PIBSI, namely the N_{SI}/N_{IB} ratio, to the ratio of the absorbances at 1705 and 1390 cm^{-1}. Using eq 3, the N_{SI}/N_{IB} ratios of *b*-PIBSI-DETA and *b*-PIBSI-TEPA were found to equal (1:31 ± 2) and (1:34 ± 2), respectively, which was different from the N_{SA}/N_{IB}

dx.doi.org/10.1021/jp5009576 | J. Phys. Chem. B 2014, 118, 3899−3911

ratio obtained for PIBSA found to equal 1:49 ± 1. The N_{SI}/N_{IB} ratio obtained by FTIR was similar to that observed by ^{1}H NMR implying that the longer PIB chains would have been selectively removed from the resulting *b*-PIBSI-TEPA product which was unlikely to have happened during the acid and base washes conducted to purify PIBSI. Consequently another procedure was applied to determine the chemical composition of the PIBSI dispersant.

$$\frac{N_{SI}}{N_{IB}} = 0.035 \times \frac{\text{abs}(1705\ \text{cm}^{-1})}{\text{abs}(1390\ \text{cm}^{-1})} \quad (3)$$

Gel Permeation Chromatography (GPC). The inconsistencies encountered in the characterization of the PIBSI dispersants when using ^{1}H NMR and FTIR spectroscopy complicated the determination of the appropriate amounts of PIBSA and polyamine that had to be placed in the reaction vessel to yield the *b*-PIBSI dispersants. Since the goal of this study was to prepare a series of *b*-PIBSI dispersants whose size should be double that of PIBSA, GPC was employed as a third characterization technique to determine which composition of PIBSA and polyamine reactants in the reaction mixture would yield the *b*-PIBSI product having the largest molecular weight and as little as possible unreacted PIBSA reactant.

The GPC trace obtained for PIBSA is shown in Figure 4. PIBSA eluted at an elution volume (V_{el}) of 27 mL. A low molecular weight impurity was found to elute at a V_{el} of 29 mL. The origin of this impurity is unknown. It did not participate in the reaction leading to the synthesis of the *b*-PIBSI dispersants as it was also found in the GPC trace of the purified product. It might represent a small fragment of unreacted PIB. Using a calibration curve based on polystyrene standards, the apparent number-averaged molecular weight M_n for PIBSA was determined to equal 1200 g/mol. M_n obtained by the direct analysis of the GPC trace was much lower than that of 2800 g/mol predicted from the N_{SA}/N_{SI} ratio of 1:49 ± 1 and 1:55 ± 2 obtained by FTIR and ^{1}H NMR, respectively, assuming that each PIBSA chain is terminated with a single SAH group. The reason for this discrepancy in M_n value can be traced back to the calibration of the GPC instrument that was conducted with polystyrene (PS) instead of PIB standards, thus yielding apparent M_n values.

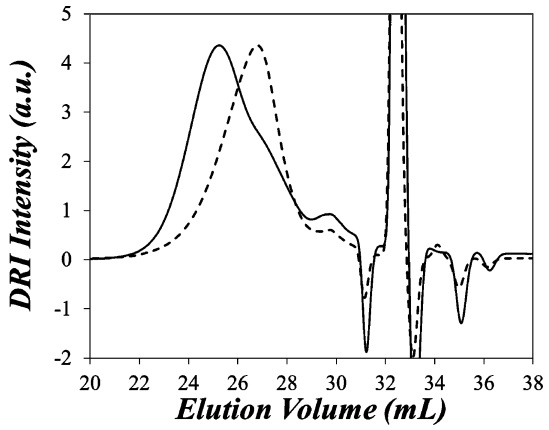

Figure 4. GPC traces of (---) PIBSA and (—) *b*-PIBSI-TEPA.

GPC analysis of the product of the reaction between 1 mol equiv of a polyamine like TEPA and 2 mol equiv of PIBSA yielded a main peak in Figure 4 that was shifted to a lower elution volume compared to PIBSA reflecting the expected increase in molecular weight. Moreover, a shoulder appeared on the right side of the main peak at elution volume of 27 mL. Similar features were observed with all *b*-PIBSI dispersants. The shoulder found at 27 mL in the GPC trace of the dispersant can be due to interactions between the packing material of the GPC column and the secondary amines of the polar core of the *b*-PIBSI dispersant. However, it was also noted that the shoulder eluted at the same position as PIBSA and could also have been unreacted PIBSA resulting from the use of an erroneous N_{SA}/N_{IB} ratio to prepare the reaction mixture with a 2:1 molar ratio of PIBSA to polyamine. This observation led to the hypothesis that GPC analysis could be used to determine the optimal reaction mixture composition that would minimize the amount of unreacted PIBSA left in the reaction product. Therefore, PIBSA was reacted with different amounts of hexamethylenediamine (HMDA) because full reaction of HMDA with PIBSA eliminates the possibility that secondary amines might adsorb onto the GPC column. The ratio of HMDA to PIBSA, namely the [HMDA]/[PIBSA] ratio expressed in mmol of HMDA per grams of PIBSA, was changed from 0.1 to 0.4.

As the [HMDA]/[PIBSA] ratio decreased from 0.4 to 0.17 mmol/g, the shoulder intensity at V_{el} = 27 mL decreased steadily until it reached a minimum value (Figure 5). However, a further decrease in the [HMDA]/[PIBSA] ratio resulted in an

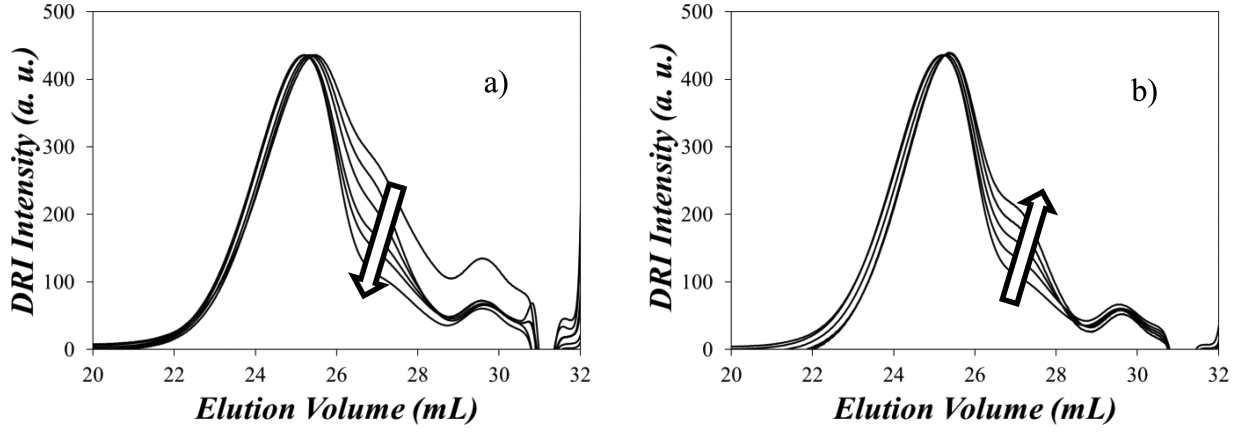

Figure 5. GPC traces of *b*-PIBSI-HMDA samples obtained from the reaction of PIBSA and HMDA. (a) [HMDA]/[PIBSA] is varied from 0.40 mmol/g (top) to 0.17 mmol/g (bottom), and (b) [HMDA]/[PIBSA] is varied from 0.17 mmol/g (bottom) to 0.10 mmol/g (top).

dx.doi.org/10.1021/jp5009576 | J. Phys. Chem. B 2014, 118, 3899−3911

increase of the shoulder intensity. The ratio of the shoulder intensity to the intensity of the main peak was calculated and plotted as a function of the [HMDA]/[PIBSA] ratio in Figure 6.

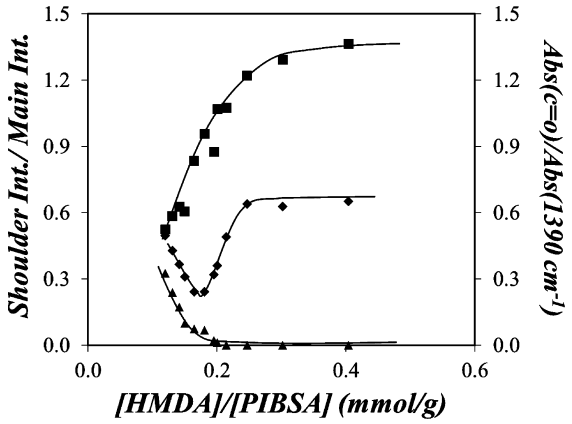

Figure 6. Plots of abs(1705 cm^{-1})/abs(1390 cm^{-1}) (■), abs(1785 cm^{-1})/abs(1390 cm^{-1}) (▲), and shoulder-to-peak intensity ratio of the GPC traces (♦) versus the [HMDA]/[PIBSA] ratio.

Low [HMDA]/[PIBSA] ratios ensured that all HMDA molecules had reacted with PIBSA so that the reaction mixture contained unreacted PIBSA and *b*-PIBSI-HMDA. As the [HMDA]/[PIBSA] ratio was further increased, less unreacted PIBSA could be found in the reaction mixture and the ratio of the shoulder-to-main peak intensities decreased in Figure 6. Although more *b*-PIBSI-HMDA was produced as more HMDA was added, the formation of some *m*-PIBSI-HMDA cannot be ruled out. Consequently, the reaction mixture must have contained some PIBSA, *m*-PIBSI-HMDA, and *b*-PIBSI-HMDA. PIBSA and *m*-PIBSI-HMDA are expected to elute at the same position in the GPC trace, but more PIBSA or *m*-PIBSI-HMDA are expected to be present in the mixture at low or high [HMDA]/[PIBSA] ratios, respectively. The plot of the ratio of the shoulder-to-main peak intensities as a function of the [HMDA]/[PIBSA] ratio indicates that *b*-PIBSI-HMDA is produced in the highest yield when the ratio passes through a minimum for an [HMDA]/[PIBSA] ratio of 0.17 mmol/g. This [HMDA]/[PIBSA] ratio corresponds to a chemical composition for PIBSA described by an N_{SA}/N_{IB} ratio of (1:52). This result agrees with the chemical composition of PIBSA determined by FTIR (1:49 ± 1) and ^{1}H NMR (1:55 ± 2) spectroscopy.

A better understanding of the nature of the functional groups that were present in the reaction mixtures was obtained by acquiring the FTIR spectra of the products recovered from the reaction mixtures at different [HMDA]/[PIBSA] ratios. Figure S4 shows the FTIR spectra acquired for the reaction mixtures obtained with [HMDA]/[PIBSA] ratios of 0.1 and 0.4 mmol/g corresponding to positions on the left and the right of the 0.17 mmol/g minimum in Figure 6. Overall, many spectral features were retained, but variations in the region of the FTIR spectra corresponding to the carbonyl functional groups were clearly visible. The absorbance band of the carbonyl shifted from 1785 to 1705 cm^{-1} when the [HMDA]/[PIBSA] ratio changed from 0.1 to 0.4 mmol/g. This behavior was monitored in all FTIR spectra and plots of the Abs(1705 cm^{-1})/Abs(1390 cm^{-1}) and Abs(1785 cm^{-1})/Abs(1390 cm^{-1}) ratios are given in Figure 6 as a function of the [HMDA]/[PIBSA] ratio. Figure 6 demonstrates that an increase in the [HMDA]/[PIBSA] ratio resulted in an increase of the absorbance at 1705 cm^{-1} indicating succinimide formation that was accompanied by a decrease of the absorbance at 1785 cm^{-1} reflecting the disappearance of the SA units. Almost all SA units had disappeared from the reaction mixture when the shoulder-to-main peak intensity ratio reached its minimum value in Figure 6 for an [HMDA]/[PIBSA] ratio of 0.17 mmol/g. For [HMDA]/[PIBSA] ratios greater than 0.17 mmol/g, the absorbance at 1785 cm^{-1} was equal to zero indicating that all PIBSA had reacted and that all SA units had been converted to succinimides. Surprisingly, the absorbance at 1705 cm^{-1} continued to increase. Since [HMDA]/[PIBSA] ratios larger than 0.17 mmol/g are expected to generate greater amounts of *m*-PIBSI-HMDA with a free primary amine, the trend shown in Figure 6 suggests that interactions due to hydrogen bond formation between the primary amine of *m*-PIBSI-HMDA and the succinimide groups of *m*-PIBSI-HMDA and *b*-PIBSI-HMDA lead to an increase in the absorbance at 1705 cm^{-1}.

In turn, this effect might be responsible for the discrepancy found by FTIR between the chemical composition of PIBSA (N_{SA}/N_{IB} = 1:49 ± 1) and the PIBSI dispersants (N_{SI}/N_{IB} = 1:33). Since hydrogen bonds are absent in the mixtures of methylsuccinimide and PIB used to generate the calibration curve given in eq 3, the absorbance at 1705 cm^{-1} is overestimated in the FTIR spectra obtained for polymer mixtures containing some *m*-PIBSI-HMDA and eq 3 yields a larger SI-content than expected from the known N_{SA}/N_{IB} ratio of PIBSA. In summary, trends obtained in Figure 6 clearly demonstrate that the ability of FTIR spectroscopy to provide qualitative information about the chemical composition of

Table 2. Summary of the Chemical Compositions of the PIBSI Dispersants As Determined by ^{1}H NMR, FTIR, GPC, and UV−Vis

dispersants	chemical composition	^{1}H NMR	FTIR (peak height)	GPC	UV−vis
PIBSA	N_{SA}/N_{IB}	1:55 ± 2	1:49 ± 1	1:52	–
m-PIBSI-$PyNH_2$	N_{SI}/N_{IB}	1:45	1:44	–	1:55 ± 1
m-PIBSI-octylamine	N_{SI}/N_{IB}	*a*	1:39	–	–
b-PIBSI-HMDA	N_{SI}/N_{IB}	1:32 ± 2	1:49 ± 2	–	–
b-PIBSI-DETA	N_{SI}/N_{IB}	1:33 ± 1	1:31 ± 2	–	–
b-PIBSI-TETA	N_{SI}/N_{IB}	1:30 ± 2	1:32 ± 1	–	–
b-PIBSI-TEPA	N_{SI}/N_{IB}	1:32 ± 1	1:34 ± 2	–	–
b-PIBSI-PEHA	N_{SI}/N_{IB}	1:33 ± 1	1:32 ± 1	–	–

[a]Small shoulder on the peak at 3.4 ppm of the ^{1}H NMR spectrum of *m*-PIBSI-Octylamine made the calculation of the N_{SI}/N_{IB} ratio inaccurate.

dx.doi.org/10.1021/jp5009576 | J. Phys. Chem. B 2014, 118, 3899−3911

PIBSI dispersants is strongly undermined when hydrogen bonds are present in the sample.

The trends shown in Figure 6 established that a reaction mixture containing 0.17 mmol of polyamine per gram of PIBSA yields a PIBSI dispersant that would contain a minimum amount of unreacted PIBSA and a maximum amount of *b*-PIBSI dispersant. Consequently, a [polyamine]/[PIBSA] ratio of 0.17 mmol/g was used to prepare all the PIBSI dispersants reported in this study. The summary of the chemical compositions determined by different techniques for all the PIBSI dispersants prepared in this study is given in Table 2.

UV−Visible Spectrophotometer. UV−vis spectroscopy was also used to further confirm the chemical composition of PIBSA and help substantiate further the proposal that interactions between the PIBSI-dispersants were responsible for the discrepancies found between the N_{SA}/N_{IB} ratios for PIBSA by FTIR, ^{1}H NMR, and GPC analysis and the N_{SI}/N_{IB} ratio found for all *b*-PIBSI dispersants by FTIR and ^{1}H NMR. To this end, PIBSA was reacted with 1-pyrenemethylamine ($PyNH_2$) to yield *m*-PIBSI-$PyNH_2$. Using the molar absorbance coefficient of 1-pyrenemethylsuccinimide in THF found to equal 44,535 M^{-1} cm^{-1} at 344 nm, the pyrene content and thus the succinimide content of *m*-PIBSI-$PyNH_2$ yielded an N_{SI}/N_{IB} ratio of 1:55 ± 1, in agreement with the N_{SA}/N_{IB} ratio of 1:52 ± 4 found for PIBSA.[29]

The advantage of using a pyrene derivative is that the absorbance of pyrene reflects the existence of pyrene−pyrene interactions.[33] This is achieved by monitoring the ratio of the peak absorbance at 343 nm to that of the adjacent trough in Figure S5 to obtain the P_A value. A P_A value of 3.0 or greater suggests that no pyrene−pyrene interactions are present. A lower P_A value indicates that pyrene aggregates exist. The absorption spectrum of a 0.14 g L^{-1} *m*-PIBSI-$PyNH_2$ solution in THF corresponding to a pyrene concentration of 0.04 mmol L^{-1} yielded a P_A value of 3.04 confirming the absence of pyrene aggregates in THF.

Since differences between the N_{SA}/N_{IB} ratio for PIBSA and the N_{SI}/N_{IB} ratio of all PIBSI-dispersants observed by ^{1}H NMR and FTIR spectroscopy were attributed to interactions between the PIBSI-dispersants, solutions of *m*-PIBSI-$PyNH_2$ were prepared under conditions that would mimic those encountered when acquiring a ^{1}H NMR and FTIR spectrum. To this end, *m*-PIBSI-$PyNH_2$ was dissolved in deuterated chloroform at a same concentration as that used for ^{1}H NMR (10 mg/mL) and the UV−vis absorption spectrum was acquired. A P_A value of 2.45 was obtained (Figure 7) suggesting the formation of *m*-PIBSI-$PyNH_2$ aggregates in deuterated chloroform. Similarly, a solid paste of *m*-PIBSI-$PyNH_2$ was applied on one of the walls of the UV−vis cell to generate a polymer film similar to that used for the FTIR experiments. The P_A value of the film was equal to 1.71 confirming that *m*-PIBSI-$PyNH_2$ aggregates are also generated in the solid state (Figure 7).

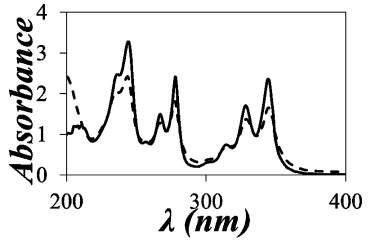

Figure 7. UV−vis absorption spectra for a 0.04 mol L^{-1} solution of *m*-PIBSI-$PyNH_2$ in d-chloroform (—) and *m*-PIBSI- $PyNH_2$ in the solid state (---).

It is noteworthy that since *m*-PIBSI-$PyNH_2$ bears no free primary amine, the *m*-PIBSI-$PyNH_2$ aggregates are induced by polar interactions between the succinimide groups in apolar chloroform and the PIB film. Although $\pi-\pi$ interactions must certainly strengthen the association between the pyrene groups once the *m*-PIBSI-$PyNH_2$ aggregates are being formed, pyrene being highly soluble in chloroform does not drive the association. The polar succinimide pendants are responsible for inducing the aggregation. The presence of residual amounts of primary and secondary amines for the PIBSI-dispersants prepared with polyamines other than HMDA increases the strength of these interactions which lead to distorted signals in the FTIR and ^{1}H NMR spectra.

Since all techniques used to characterize the chemical composition of PIBSA converged on an N_{SA}/N_{IB} ratio of 1:52 ± 4 for PIBSA corresponding to a chemical composition of 0.34 mmol of SA units per gram of PIBSA, reaction mixtures containing 0.17 mmol of polyamine per gram of PIBSA were used to conduct the synthesis of all the *b*-PIBSI dispersants prepared in this study. The experiments conducted so far indicate that the characterization of the chemical composition of *b*-PIBSI-dispersants by FTIR and ^{1}H NMR spectroscopy is challenging since aggregation of the succinimide moieties promoted by the presence of amines distorts the ^{1}H NMR and FTIR spectra. This conclusion led us to investigate whether another technique would be better suited to determine the chemical composition of *b*-PIBSI-dispersants. Since the *b*-PIBSI-dispersants contain two fluorescent succinimide moieties and a number of secondary amines that are efficient quenchers of fluorescence, fluorescence quenching experiments were conducted on the *b*-PIBSI dispersants to determine whether the fluorescence signal of the succinimide units would be sensitive to the number of secondary amines in the polyamine core.

Steady-State and Time-Resolved Fluorescence Measurements. The intrinsic fluorescence of PIBSA and some PIBSI dispersants has already been reported.[32] Since secondary and primary amines are known to be efficient fluorescent quenchers,[34] we investigated whether fluorescence experiments would provide information about the chemical composition of the PIBSI dispersants. To determine the best excitation and emission wavelengths to monitor the fluorescence of PIBSA and the *b*-PIBSI dispersants, the fluorescence spectra of these polymers were acquired at excitation wavelengths selected in the 250−420 nm range. The fluorescence spectra of the polymer solutions in THF were broad and structureless. For all samples, the emission shifted to higher wavelengths as the excitation wavelength was increased past 360 nm (Figure 8). This behavior indicates that PIBSA and the *b*-PIBSI dispersants contain more than one chromophore and that changing the excitation wavelength enables the photoselection of different chromophores. Since the *b*-PIBSI dispersants contained a fluorescent succinimide group, the fluorescence of the *b*-PIBSI dispersants was also compared to that of *N*-methylsuccinimide (*N*-MSI). Excitation of *N*-MSI at different wavelengths resulted in a set of fluorescence spectra centered around the same emission wavelength confirming the excitation of a single chromophore. The position (λ_{max}) and fluorescence intensity (I_{max}) at the fluorescence maximum were recorded and plotted on a same figure as a function of the excitation wavelength (λ_{ex})

dx.doi.org/10.1021/jp5009576 | J. Phys. Chem. B 2014, 118, 3899−3911

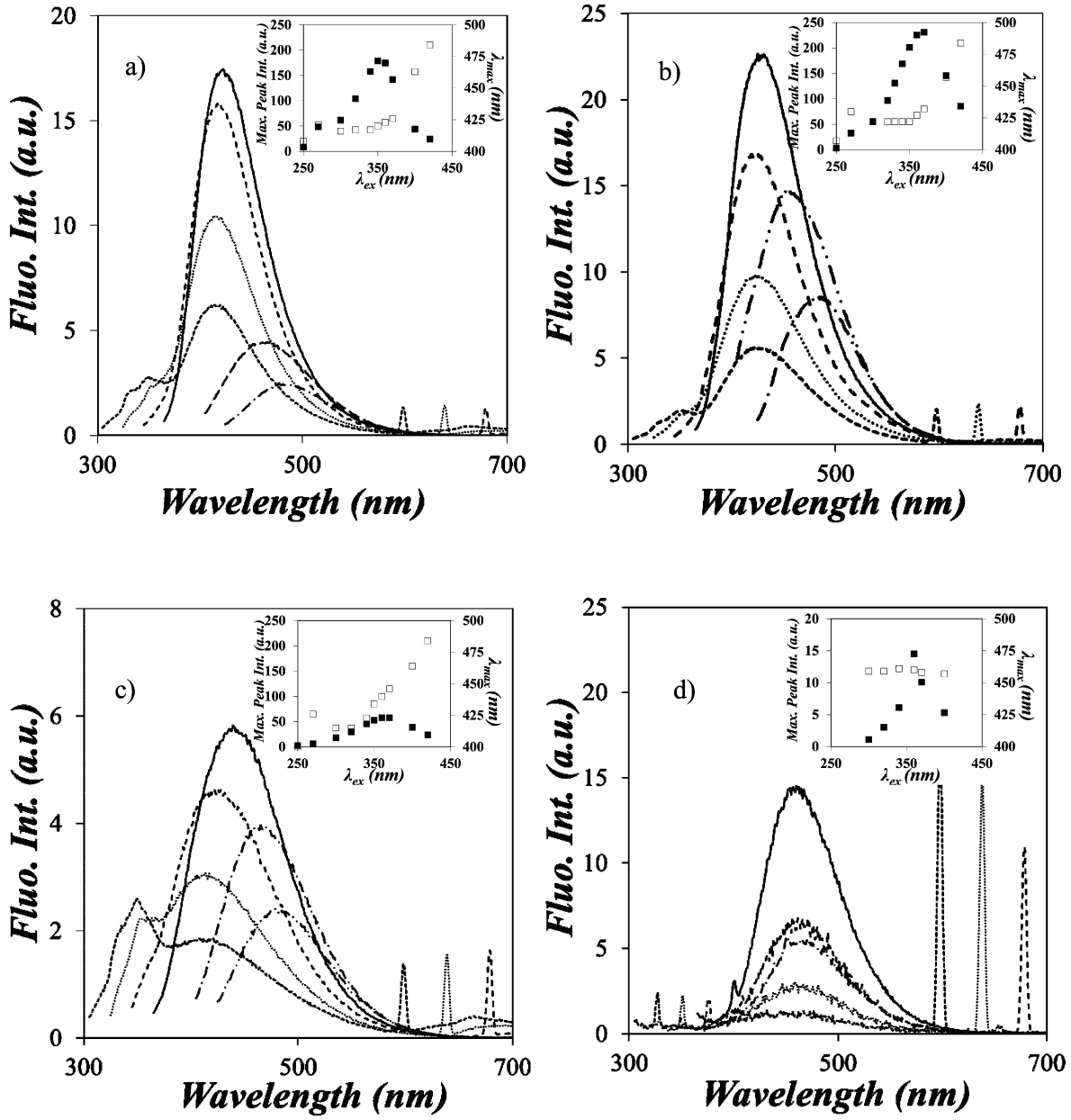

Figure 8. Steady-state fluorescence spectra of (a) PIBSA (8 g/L), (b) *b*-PIBSI-HMDA (8 g/L), (c) *b*−PIBSI−PEHA (8 g/L), and (d) *N*-methyl succinimide (0.45 mol/L). Key: (----) λ_{ex} = 300 nm, (···) λ_{ex} = 320 nm, (- - -) λ_{ex} = 340 nm, (——) λ_{ex} = 360 nm, (−− −) λ_{ex} = 400 nm, and (−− − −) λ_{ex} = 420 nm in THF. Insert: Maximum peak intensity (I_{max}) (■) and maximum peak intensity wavelength (λ_{max}) (□) versus excitation wavelength (λ_{ex}).

as shown in the inset of Figure 8. For all *b*−PIBSI dispersants, as λ_{ex} increased, λ_{max} remained constant within experimental error and equal to 423 ± 5 for all samples before increasing rapidly with increasing λ_{ex} for λ_{ex} greater than 360 nm. This behavior suggests that a main chromophore is photoselected for λ_{ex} values between 300 and 360 nm, and that other chromophores are being excited at higher λ_{ex}. For all *b*-PIBSI dispersants, the fluorescence intensity at the fluorescence maximum (I_{max}) in the fluorescence spectrum increased steadily with increasing λ_{ex} until it passed through a maximum at λ_{ex} = 360 nm. For λ_{ex} greater than 360 nm, I_{max} decreased continuously with increasing λ_{ex}. The behavior of I_{max} as a function of λ_{ex} is the result of a number of effects such as changes in the molar absorbance coefficient of the chromophore in this range of λ_{ex} values. Together the trends shown in Figure 8 suggest that excitation of the solutions of dispersant in THF yields a maximum fluorescence signal when excited at 360 nm. Consequently, this excitation wavelength was used for all experiments thereafter.

Although a maximum in fluorescence intensity was found upon exciting the solutions of PIBSA and all *b*-PIBSI dispersants at λ_{ex} = 360 nm, it was noticeable that the fluorescence of the PIBSA solution was blue-shifted and weaker than that of the *b*-PIBSI-HMDA solution. Overlaying the fluorescence spectra of the 8 g/L solutions of *b*-PIBSI-HMDA, *b*-PIBSI-DETA, *b*-PIBSI-TETA, *b*-PIBSI-TEPA, and *b*-PIBSI-PEHA in Figure 9 clearly showed that the fluorescence intensity decreased with increasing number of secondary amines in the polyamine linker of the dispersant. Since secondary amines are known to be efficient fluorescence quenchers.[33,34] the trends

dx.doi.org/10.1021/jp5009576 | J. Phys. Chem. B 2014, 118, 3899−3911

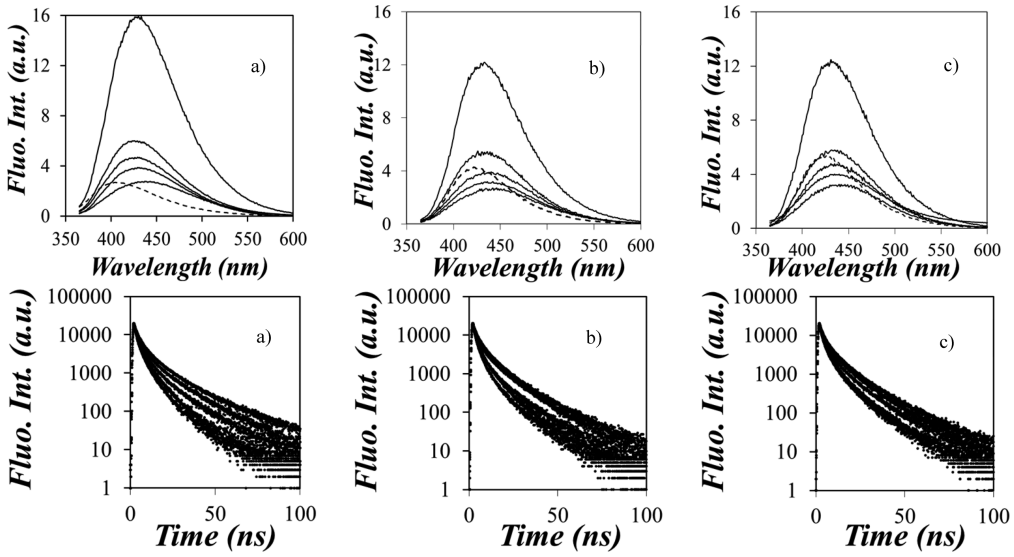

Figure 9. Top: Steady-state fluorescence spectra of (- - -) PIBSA and (—) *b*-PIBSI dispersants. Bottom: Time-resolved fluorescence decays. From top to bottom: *b*-PIBSI-HMDA, *b*-PIBSI-DETA, *b*-PIBSI-TETA, *b*-PIBSI-TEPA, and *b*-PIBSI-PEHA in (a) dodecane, (b) THF, and (c) dodecanone (C_{PIBSI} = 8 g/L, λ_{ex} = 360 nm, and λ_{em} = 428 nm).

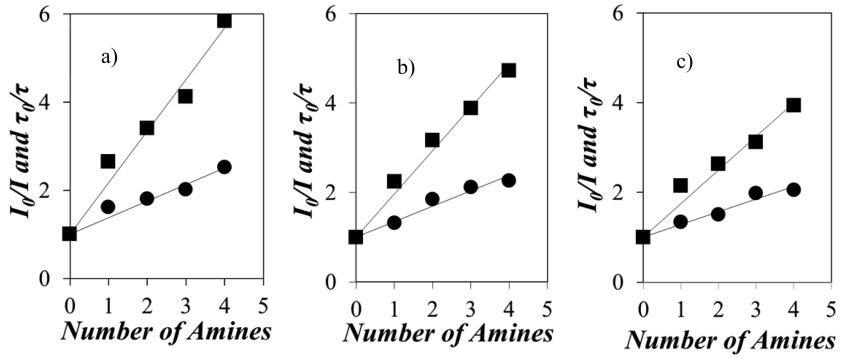

Figure 10. Stern–Volmer plot for the quenching of *b*-PIBSI dispersants by secondary amines in (a) dodecane, (b) THF, and (c) dodecanone.

shown in Figure 9 indicate that *b*-PIBSI-HMDA with no secondary amine and *b*-PIBSI-PEHA with four secondary amines yield the highest and lowest fluorescence intensity, respectively. In turn, this photophysical effect might be beneficial to infer the chemical composition of a given *b*-PIBSI dispersant by comparing the decrease of its fluorescence intensity to that of *b*-PIBSI-HMDA. As a result, the photophysical properties of the series of *b*-PIBSI dispersants listed in Table 2 were investigated.

The information contained in Figure 9 can be summarized by plotting the ratio of the fluorescence intensity of the unquenched emitter (i.e., *b*-PIBSI-HMDA) over that of the quenched emitters (i.e., the other *b*-PIBSI dispersants), namely the I_0/I ratio, as a function of the number of secondary amines found in the polyamine linker. This was done in Figure 10. Within experimental error, the I_0/I ratio was found to increase linearly with increasing number of secondary amines.

More information about the nature of fluorescence quenching, particularly whether it is static, dynamic, or a mixture of both, can be obtained by conducting time-resolved fluorescence measurements. To this end, the fluorescence decays of the *b*-PIBSI dispersants were acquired using an excitation and emission wavelengths of 360 and 428 nm, respectively. The corresponding fluorescence decays are shown in Figure 9. They were all strongly multiexponential. The decays were fitted with a sum of three-to-four exponentials and the number-average lifetime was determined ($\tau = \sum_{i=1}^{n} a_i\tau_i / \sum_{i=1}^{n} a_i$). The pre-exponential factors and decay times retrieved from this analysis are provided in the Supporting Information (Tables S1–S4). The ratio τ_o/τ, where τ_o and τ are, respectively, the number-average lifetime in the absence and presence of secondary amines in the polyamine linker, was plotted as a function of the number of secondary amines in Figure 10. Here again, a linear increase in τ_o/τ, with increasing number of secondary amines was observed. The ratios I_0/I and τ_o/τ did not overlap however indicating that static quenching is taking place.

Static quenching occurs when associations between fluorophore and quencher are present. These associations are likeliest to happen when secondary amines and fluorophores are located in close proximity within the macromolecule, again strongly suggesting that the succinimide moieties of the *b*-PIBSI dispersants are responsible for the fluorescence of the *b*-PIBSI dispersants centered at 423 ± 5 nm when exciting the solution at 360 nm. If one considers the volume V_{core} defined by the two succinimide moieties and the polyamine linker, increasing the number of secondary amine quenchers in the polyamine spacer increases the local concentration of secondary amines in V_{core} and thus, the efficiency of quenching as observed Figure 10.

dx.doi.org/10.1021/jp5009576 | J. Phys. Chem. B 2014, 118, 3899–3911

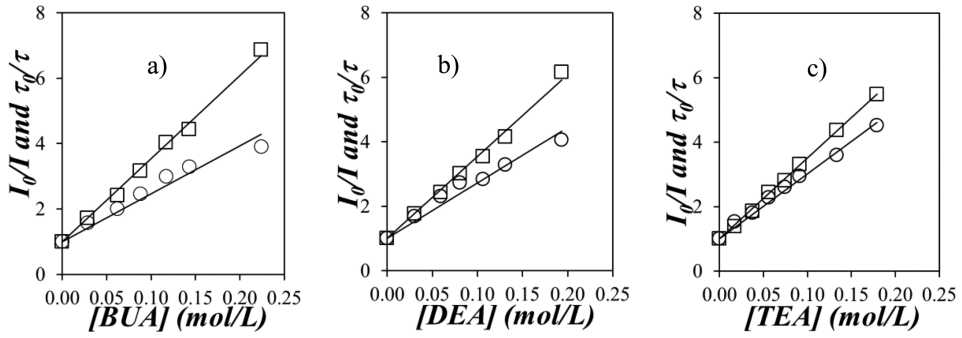

Figure 11. Stern−Volmer plot for the quenching of *N*-MSI by (a) BUA, (b) DEA, and (c) TEA in THF.

The ability of amines at quenching the fluorescence of the succinimide units was confirmed by monitoring the quenching of *N*-MSI by butylamine (BUA), diethylamine (DEA), and triethylamine (TEA) in THF. As shown in Figure S6, the fluorescence intensity of *N*-MSI decreased strongly with increasing concentration of BUA, DEA, and TEA. Dynamic fluorescence quenching of *N*-MSI was also apparent in the fluorescence decays of *N*-MSI presented in Figure S6 that show a faster decay of *N*-MSI with increasing BUA, DEA, and TEA concentration. With the data collected for *N*-MSI in Figures S5 and S6, the I_0/I and τ_o/τ ratios were determined and plotted as a function of BUA, DEA, and TEA concentrations in Figure 11. The trends obtained for the I_0/I and τ_o/τ ratios in Figure 11 are similar to those obtained with the *b*-PIBSI dispersants, the ratios showing a linear increase with increasing BUA, DEA, and TEA concentration. With all three amines, the I_0/I ratio took larger values than the τ_o/τ ratio demonstrating the existence of static quenching. The only difference between the plots shown in Figure 10 and Figure 11 is that quenching occurs intramolecularly with the *b*-PIBSI dispersants and intermolecularly with *N*-MSI. The similarity of the trends obtained strongly suggests that the secondary amines in the polyamine linker of the *b*-PIBSI dispersants are quenching the fluorescent succinimide moieties connecting PIB to the polyamine.

In order to describe the quenching experiments more quantitatively, Scheme 3 was introduced. In Scheme 3, a chromophore *M* forms a complex *MQ* in the presence of a quencher molecule *Q* with an equilibrium constant K_S. Absorption of a photon by the uncomplexed chromophore *M* present in solution with a molar fraction *f* generates the excited species *M** which can either fluoresce with a lifetime τ_o or be quenched by diffusive encounter with *Q* with a rate constant k_Q. A molar fraction $1 - f$ of the chromophore *M* is also present in the form of the complex *MQ* in the solution. Excitation of the complex *MQ* results in no fluorescence as the excited chromophore *M** is quenched instantaneously due to its complexation with *Q*. Scheme 3 yields eqs 4 and 5 that describe the τ_o/τ and I_0/I ratios, respectively.

Scheme 3. Photophysical Processes Undergone by Chromophore M Subject to Static and Dynamic Quenching[35]

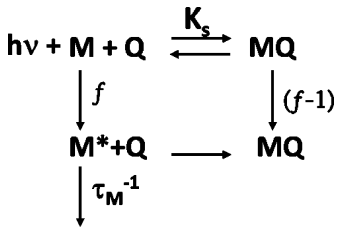

The quencher concentration [Q] in eqs 4 and 5 represent either the local concentration of secondary amines in the volume defined by the polyamine linker of the *b*-PIBSI dispersants or the concentration of BUA, DEA, and TEA in the *N*-MSI solution. The product $k_Q \times \tau_o$ represents the efficiency of dynamic quenching. It will be referred to as K_D ($=k_Q \times \tau_o$) hereafter. Using this nomenclature, the slope of the plot between the I_0/I ratio and [Q] yields the sum K_{app} ($=K_S + K_D$) whereas the slope of the plot between the τ_o/τ ratio and [Q] yields K_D. Consequently, the constants K_S and K_D could be estimated from the slope of the straight lines shown in Figures 10 and 11. Their values are listed in Tables 3 and 4.

$$\frac{\tau_0}{\tau} = 1 + k_Q\tau_0 \times [Q] \tag{4}$$

$$\frac{I_0}{I} = 1 + (K_S + k_Q\tau_0) \times [Q] + K_S k_Q \tau_0 \times [Q]^2 \approx 1 + (K_S + k_Q\tau_0) \times [Q] \tag{5}$$

The quenching experiments were conducted in dodecane, dodecanone, and THF for the *b*-PIBSI dispersants. In the case of *b*-PIBSI in THF and dodecane, $K_S/(K_S + K_D)$ is about twice larger than $K_D/(K_S + K_D)$ demonstrating the importance of static quenching in these experiments. Introduction of a carbonyl group by using dodecanone instead of dodecane reduces the ability of the secondary amines to bind to the succinimides. As expected, the $K_S/(K_S + K_D)$ ratio decreased from 0.68 ± 0.01 in dodecane to 0.58 ± 0.02 in dodecanone.

Because of solubility issues in dodecane and dodecanone, quenching of *N*-MSI by BUA, DEA, and TEA was solely conducted in THF. In the case of BUA and DEA, the $K_S/(K_S + K_D)$ ratio took values of 0.36 ± 0.00 and 0.30 ± 0.00,

Table 3. τ_0, K_D, and K_s Values Derived from the Stern−Volmer Plots Shown in Figure 11

name	solvent	τ_0 (ns)	K_D	K_S	K_S/K_{app}	K_D/K_{app}
b-PIBSI	dodecane	4.8	0.38 (±0.00)	0.82 (±0.01)	0.68 (±0.01)	0.32 (±0.00)
b-PIBSI	THF	4.4	0.34 (±0.01)	0.63 (±0.01)	0.65 (±0.01)	0.35 (±0.01)
b-PIBSI	dodecanone	4.5	0.29 (±0.01)	0.41 (±0.01)	0.58 (±0.02)	0.42 (±0.01)

dx.doi.org/10.1021/jp5009576 | J. Phys. Chem. B 2014, 118, 3899−3911

Table 4. Data Obtained from Stern−Volmer Plot with *N*-MSI in the Presence of BUA, DEA, and TEA in THF

name	τ_0 (ns)	k_Q (M^{-1} ns^{-1})	K_D (M^{-1})	K_S (M^{-1})	K_S/K_{app}	K_D/K_{app}
N-MSI + BUA	10.1	3.93 (±0.00)	16.00 (±0.01)	25.14 (±0.02)	0.36 (±0.00)	0.64 (±0.00)
N-MSI + DEA	10.1	4.74 (±0.02)	17.44 (±0.02)	25.17 (±0.01)	0.30 (±0.00)	0.70 (±0.00)
N-MSI + TEA	10.1	5.18 (±0.00)	22.81 (±0.00)	25.08 (±0.02)	0.09 (±0.00)	0.91 (±0.00)

respectively. The $K_S/(K_S + K_D)$ value was slightly higher for BUA in comparison to DEA probably due to the ability of BUA to H-bond more strongly to *b*-MSI. Interestingly, the $K_S/(K_S + K_D)$ ratio decreased from 0.36 ± 0.00 for BUA to 0.09 ± 0.00 for TEA which could not H-bond with *b*-MSI, thus confirming the nature of the interactions between the succinimides and the secondary and primary amines. Finally, k_Q was found to increase according to the sequence BUA < DEA< TEA.

The results obtained thus far suggest that the fluorescent succinimide moieties constituting the *b*-PIBSI dispersants are quenched efficiently by secondary amines. Hydrogen bonding between the succinimide carbonyls and the secondary amine protons leads to static quenching whose magnitude increases linearly with the number of secondary amines present in the polyamine linker joining two PIB chains.

The linear relationship found to exist between the I_0/I and τ_0/τ ratios and the moles of secondary amines in the polyamine spacer of the *b*-PIBSI dispersants is expected to provide a novel analytical method toward the characterization of the chemical composition of *b*-PIBSI dispersants. On the basis of the linear Stern−Volmer plot shown in Figure 10, the amines content of an unknown *b*-PIBSI dispersant can now be determined by measuring its fluorescence intensity I and average lifetime τ and comparing them to the corresponding I_0 and τ_o values obtained with *b*-PIBSI-HMDA dispersant prepared with the same PIBSA unit used to prepare the unknown *b*-PIBSI dispersant.

CONCLUSIONS

The chemical composition of several PIBSI dispersants prepared with different molar ratios of PIBSA and hexamethylene diamine was characterized quantitatively by using a combination of GPC and FTIR analysis. This study confirmed that the existence of hydrogen bonds between the secondary amines of the polyamine spacer and the succinimide carbonyls of *b*-PIBSI dispersants represents a serious impediment to the characterization of the chemical composition of these dispersants by standard ^{1}H NMR and FTIR spectroscopies. By contrast, the procedure combining GPC and FTIR analysis enabled the determination of appropriate reaction conditions to prepare a series of five *b*-PIBSI dispersants with polyamine linkers having a well-defined number of secondary amines.

Having established that techniques such as ^{1}H NMR and FTIR provide unreliable information about the chemical composition of *b*-PIBSI dispersants, steady-state and time-resolved fluorescence quenching experiments were carried out on the five *b*-PIBSI dispersants prepared with a known number of secondary amines in the polyamine linker to investigate whether the fluorescence emitted by the succinimide groups present in the *b*-PIBSI dispersants would respond to the number of secondary amines of a given *b*-PIBSI dispersant. As the number of secondary amines was increased in the polyamine linker used to prepare the dispersants, the fluorescence intensity I and average lifetime τ of the *b*-PIBSI dispersants were found to decrease. Stern−Volmer plots of the ratios I_0/I and τ_o/τ as a function of the number of secondary amines showed a linear behavior suggesting that fluorescence quenching measurements can provide a reliable measure of the secondary amine content of a given *b*-PIBSI dispersant. This result should be of high practical interest to scientists involved in the design of dispersants used as oil-additives.

ASSOCIATED CONTENT

Supporting Information

FTIR spectra of the PIBSI dispersants, ^{1}H MNR spectrum of methyl succinic anhydride, absorption spectrum of *m*-PIBSI-PyNH$_2$ in THF, fluorescence spectra and decays of *N*-methyl succinimide with different quenchers in THF, and tables of pre-exponential factors and decay times retrieved from the analysis of the fluorescence decays with a sum of exponentials. This material is available free of charge via the Internet at http://pubs.acs.org.

AUTHOR INFORMATION

Corresponding Author

*(J.D.) E-mail: jduhamel@uwaterloo.ca.

Notes

The authors declare no competing financial interest.

ACKNOWLEDGMENTS

The authors thank Imperial Oil and NSERC for their generous financial support of this research.

REFERENCES

(1) Rudnik, L. R. Lubricant Additives. In *Chemistry and Application*; Barbadsz, E. A., Lamb, G. D., Eds.; CRC Press: Boca Raton, FL, 2003; pp 458−490.

(2) Mortier, R. M.; Malcolm, F. F.; Orszulik, S. T. In *Chemistry and Technology of Lubricants*; Springer: London, 2009.

(3) Jao, T. C.; Passut, C. A. In *Part D: Formulation, Surfactant Science Series*; Showell, M. S., Ed.; Handbook of Detergents; CRC Press: Boca Raton: FL, 2006; pp 437−471.

(4) Wollenberg, R. H.; Rafael, S.; Plavac, F. Modified Succinimides. US Patent4,612,132, 1986.

(5) Gwinn, M. R.; Vallyathan, V. Nanoparticles: Health Effects - Pros and Cons. *Environ. Health Perspect.* **2006**, *114*, 1818−1825.

(6) Farnlund, J.; Holman, C.; Kageson, P. Emissions of Ultrafine Particles from Different Types of Light Duty Vehicles. *Eur. Env. News Info. Serv.* **2001**, *10*, 1−22.

(7) Wood, J. Canadian Environmental Indicators-Air Quality. *Stud. Environ. Policies, Fraser Inst.* **2012**, 1−69.

(8) Reisch, M. S. Tough Diesel Rule Fuels Opportunity. *Chem. Eng. News* **2005**, *5*, 20−22.

(9) Aldajah, S.; Ajayi, O. O.; Fenske, G. R.; Goldblatt, I. L. Effect of Exhaust Gas Recirculation (EGR) Contamination of Diesel Engine Oil on Wear. *Wear* **2007**, *263*, 93−98.

(10) Tomlinson, A.; Scherer, B.; Karakosta, E.; Oakey, M.; Danks, T. N.; Heyes, D. M.; Taylor, S. E. Adsorption Properties of Succinimide Dispersants on Carbonaceous Substrates. *Carbon* **2000**, *38*, 13−28.

(11) Tomlinson, A.; Danks, T. N.; Heyes, D. M.; Taylor, S. E.; Moreton, D. J. Interfacial Characterization of Succinimide Surfactants. *Langmuir* **1997**, *13*, 5881−5893.

(12) Forbes, E. S.; Neustadter, E. L. The Mechanism of Action of Polyisobutenyl Succinimide Lubricating Oil Additives. *Tribology* **1972**, *5*, 72−77.

(13) Atta, A. M.; El-Ghazawy, R. A. M.; Farag, R. K.; Abdel-Azim, A.-A. A. Crosslinked Reactive Macromonomers Based on Polyisobutylene and Octadecyl Acrylate Copolymers as Crude Oil Sorbers. *React. Funct. Polym.* **2006**, *66*, 931−943.
(14) Lee, P. T. C.; Chiu, C.-W.; Lee, T.-M.; Chang, T.-Y.; Wu, M.-T.; Cheng, W.-Y.; Kuo, S.-W.; Lin, J.-J. First Fabrication of Electrowetting Display by Using Pigment-in-Oil Driving Pixels. *ACS Appl. Mater. Interfaces* **2013**, *5*, 5914−5920.
(15) Hsu, C.-P.; Chang, L.-Y.; Chiu, C.-W.; Lee, P. T. C.; Lin, J.-J. Facile Fabrication of Robust Superhydrophobic Epoxy Film with Polyamine Dispersed Carbon Nanotubes. *ACS Appl. Mater. Interfaces* **2013**, *5*, 538−545.
(16) Le Suer, W. M.; Norman, G. R. Reaction Product of High Molecular Weight Succinic Acids and Succinic Anhydrides with an Ethylene Polyamine. US Patent3,172,892, 1967.
(17) Stuart, A. F.; Orinda, R. G.; Anderson, N.; Drummond, A. Y. Alkenyl Succinimides of Tetraethylene Pentamine. US Patent 3,202,678, 1965.
(18) Myers, D. In *Surfactant Science and Technology*; John Wiley & Sons: Hoboken, NJ, 2006.
(19) Le Suer, W. M.; Norman, G. R. Fire Resistant Hydraulic Fluid. US Patent3,272,747, 1966.
(20) Mark, E. J.; Ermama, B.; Eirich, F. R. In *Science and Technology of Rubber*; Elsevier: Akron, OH, 2005.
(21) Tessier, M.; Marechal, E. Synthesis of A-Phenyl-Ω-Anhydride Oligoisobutylene and A,Ω-Dianhydride Oligoisobutylene. *Eur. Polym. J.* **1990**, *26*, 499−508.
(22) Shen, Y.; Duhamel, J. Micellization and Adsorption of a Series of Succinimide Dispersants. *Langmuir* **2008**, *24*, 10665−10673.
(23) Dubois-Clochard, M. C.; Durand, J. P.; Delfort, B.; Gateau, P.; Barré, L.; Blanchard, I.; Chevalier, Y.; Gallo, R. Adsorption of Polyisobutenylsuccinimide Derivatives at a Solid-Hydrocarbon Interface. *Langmuir* **2001**, *17*, 5901−5910.
(24) Tessier, M.; Maréchal, E. Synthesis of Mono and Difunctional Oligoisobutylenes-III. Modification of a-Chlorooligoisobutylene by Reaction with Maleic Anhydride. *Eur. Polym. J.* **1984**, *20*, 269−280.
(25) Wollenberg, R. H.; Rafael, S.; Plavac, F. Modified Succinimide. USP 4802893, 1989.
(26) Harrison, J. J.; Ruhe, W. R. Fuel Compositions Having Polyalkylene Succinimides and Preparation Thereof. US Patent 5,853,434, 1998.
(27) Walch, E.; Gaymans, R. J. Telechelic Polyisobutylene with Unsaturated End Groups and with Anhydride End Groups. *Polymer* **1994**, *35*, 1774−1778.
(28) Mathew, A. K.; Duhamel, J.; Gao, J. Maleic Anhydride Modified Oligo(Isobutylene): Effect of Hydrogen Bonding on its Associative Strength in Hexane Characterized by Fluorescence Spectroscopy. *Macromolecules* **2001**, *34*, 1454−1469.
(29) Sippel, T. O. Microfluorometric Analysis of Protein Thiol Groups with a Coumarinylphenylmaleimide. *J. Histochem. Cytochem.* **1981**, *29*, 1377−1381.
(30) Phelan, J. C.; Sung, C. S. P. Fluorescence Characteristics of Cure Products in Bis(Maleimide)/Diallylbisphenol A Resin. *Macromolecules* **1997**, *30*, 6837−6844.
(31) Kanaoka, Y.; Machida, M.; Ban, Y.; Takamitsu, S. Fluorescence and Structure of Proteins as Measured by Incorporation of Fluorophore. II. Synthesis of Maleimide Derivatives as Fluorescence-Labeled Protein-Sulfhydryl Reagents. *Chem. Pharm. Bull.* **1967**, *15*, 1738−1743.
(32) Pucci, A.; Rausa, R.; Ciardelli, F. Aggregation-Induced Luminescence of Polyisobutene Succinic Anhydrides and Imides. *Macromol. Chem. Phys.* **2008**, *209*, 900−906.
(33) Winnik, M. A.; Bystryak, S. M.; Liu, Z.; Siddiqui, J. Synthesis and Characterization of Pyrene-Labeled Poly(Ethylenimine). *Macromolecules* **1998**, *31*, 6855−6864.
(34) Lakowicz, J. R. *Principles of Fluorescence Spectroscopy*; Plenum Press: Baltimore, MD, 1986.
(35) Winnik, F. M. Photophysics of Pre-associated Pyrenes in Aqueous Polymer Solutions and in Other Organized Media. *Chem. Rev.* **1993**, *93*, 587−614.